

INFLUENCE OF DIFFERENT VARIABLES ON THE DISSOLUTION BEHAVIOR OF CARVEDILOL FROM LIQUISOLID COMPACTS USING RESPONSE SURFACE METHODOLOGY

K. M. EL-SAY^{a,b,*}, O. A. A. AHMED^{a,c}, H. M. ALDAWSARI^a,
S. M. BADR-ELDIN^{a,d}

^aDepartment of Pharmaceutics, Faculty of Pharmacy, King Abdulaziz University, Jeddah, Saudi Arabia

^bDepartment of Pharmaceutics and Industrial Pharmacy, Faculty of Pharmacy, Al-Azhar University, Cairo 11651, Egypt

^cDepartment of Pharmaceutics and Industrial Pharmacy, Faculty of Pharmacy, Minia University, Minia, Egypt

^dDepartment of Pharmaceutics and Industrial Pharmacy, Faculty of Pharmacy, Cairo University, Cairo, Egypt

The study aimed to enhance the dissolution behavior of carvedilol (CRV) as a model of weakly basic API (BCS Class II) through its formulation in liquisolid compacts (LSCs). Fifteen formulations of LSCs were prepared utilizing one of three nonvolatile solvents namely; PEG 200, Tween 20, or PVP/VA73 and evaluated for their quality attributes. The pure CRV and CRV-LSCs were examined by differential scanning calorimetry, powder X-ray diffraction and Fourier transform infrared spectroscopy. Design of experiments was used to statistically explore the effect of the investigated variables on the dissolution behavior of CRV from the LSCs in comparison to the conventional directly compressed tablets at three different pH values. Mathematical modeling of data was carried out by computing the dissolution rate in the first 10 min (DR_{10}) and the dissolution efficiency through 60 min ($DE_{60\%}$). The results of the study indicated that DR_{10} and $DE_{60\%}$ of the optimized LSCs showed considerable faster and enhanced drug release than those of conventional tablets. The computed f_2 value was 8.23 indicating significant difference of LSCs dissolution profile compared with conventional tablets i.e. marked dissolution enhancement of CRV. The study concluded that the LS technique is a promising method to enhance the dissolution of poorly water-soluble drugs.

(Received May 18, 2019; Accepted October 8, 2019)

Keywords: Angina pectoris, Carvedilol, hypertension, In vitro dissolution, Liquisolid compacts, pH-dependent solubility, Box-Behnken design

1. Introduction

Carvedilol (CRV) is an antihypertensive β -adrenergic blocker [1,2]. It suffers a low absolute bioavailability in humans (approximately 30%). The low bioavailability of CRV is attributed to its lower solubility and extensive hepatic metabolism [3,4]. CRV is selected as a model BCS Class 2 API and is weakly basic (pKa 7.8) in which the dissolution is the rate-limiting step of the absorption of these drugs.

Various approaches have been employed to enhance the solubility and the dissolution of this class of drugs like complexation with cyclodextrin [5,6], or adsorption onto porous and nonporous large surface area carriers such as silica [7]. Several methods have been used to incorporate CRV in different formulations as solid lipid nanoparticles,[8–10] solid self-nanoemulsifying drug delivery systems [4], nasal microspheres [11], transdermal films [12], proniosomal transdermal gel [13], mucoadhesive buccal patch [14], orodispersible tablets [15], gastro retentive floating tablets [16–

*Corresponding author: kelsay1@kau.edu.sa

18], floating microspheres [19,20] to enhance its aqueous solubility and avoid the hepatic metabolism and subsequently improve its bioavailability.

It is supposed that enhanced bioavailability of drugs with limited solubility might be attained when the drug is existing in solution [21,22]. LSCs can be utilized to incorporate water-insoluble drugs in non-volatile solvents and then blending the liquid drug with special powder substrates known as the carrier with high porosity and coating materials with high adsorption capacity. The liquid medication converted into a free-flowing powder that can be compressed readily [23–26]. When this powder blend holding the drug in a solubilized liquid state is compressed into tablets, the dissolution profile was improved because of increased wettability of drugs [27,28].

LSCs reveal benefits such as simple processing, low costs compared to soft gelatin capsules, and superior drug release. The main advantage is greater bioavailability of the liquid drug produced by a huge surface area available for absorption. The study attempts to elucidate specific aspects associated with the formulation of LSCs and the variables influenced the processing and dosage form evaluation.

2. Materials and methods

2.1. Materials

Carvedilol (CRV) was gifted from Riyadh pharma (Riyadh, Saudi Arabia), Propylene glycol (PG) was bought from Fluka (Steinheim, Germany), Span 80 from Aldrich (Steinheim, Germany), Tween 20 from Medex (UK), Glycerin from Crescent Diagnostics (Jeddah, Saudi Arabia), methanol and polyethylene glycol (PEG) 400 from BDH laboratory reagents (Poole, England), PEG 200 from Merck-Schuchardt (Hohenbrunn, Germany), polyvinylpyrrolidone/vinylacetate (PVP/VA 50/50 w/w) 73, 64, and 37, all PVP/VAs were gifted from Shanghai yuking water soluble material Tech. Co. Ltd (Shanghai, China). Microcrystalline cellulose (Avicel PH 101) from Fluka (Hach Lange, Ireland), Methocel® E5 premium LV from Dow Chemical Company (Midland, MI) Silica bought from Aldrich (Steinheim, Germany), Magnesium trisilicate, sodium starch glycolate (Explotab) from JRS PHARMA GmbH & Co. KG (Rosenberg, Germany), talc from Holyland (Saudi Arabia), mannitol from Winlab (Market Harborough, UK), Methocel (hydroxypropyl methylcellulose) E5 Premium LV (HPMC E5) was purchased from Dow Chemical Company (Midland, MI).

2.2. Solubility studies

CRV solubility was determined based on the previously published works [28,29] in glycerin, PG, PEG 200, PEG 400, Span 80, Tween 20, PVP/VA 73, PVP/VA 64, and distilled water. Saturating each solvent with CRV then analyzing CRV concentration spectrophotometrically. CRV was mixed in 10 ml vials with the same amount of each of the previously mentioned solvents to generate a supersaturated system of the drug. The mixture was shaken in a water bath (GFL type 1083, Germany) for 48 hours at room temperature. Mixtures were centrifuged at 15,000 rpm for 30 minutes (Sigma type 3k30, Germany) and filtered (0.2 µm, Millipore) and then analyzed for CRV concentration spectrophotometrically at 242.5 nm (UV-Vis spectrophotometer, Jenway 67 series).

2.3. Determination of the excipients holding capacity

The excipient liquid holding capacity was determined [24,30]. Briefly, different weights of the selected liquids from 0.5 g to 2.5 g were triturated, in a mortar, after each addition with constant weight (5 g) of powder excipient. The addition of powder was continued until mortar contents transformed into dry powder. This procedure was carried out by the addition of fumed silica to explore the effect of fumed silica on improving the flow behavior of the powder blends. Liquid load factor (Lf) was calculated by dividing the liquid medication weight (w) to the carrier powder weight (Q) in the system (i.e. $Lf = W/Q$).

2.4. Pre-compression evaluation of the prepared liquisolid powders

2.4.1. Evaluation of flow and packing properties

The flowability of the prepared mixtures was studied either by direct technique through the determination of the angle of repose (Equation 1), or with the indirect method by calculation of both Hausner ratio (Equation 2) and Carr's index (Equation 3) after measuring the bulk and tap densities of the LSCs.[31] Each sample had a constant amount of Avicel (5 g) and an increasing amount of the solvent ascendingly from 0.5g – 2.5g (trial 1-5).

$$\text{Angle of repose } (\theta) = \tan^{-1} (\text{Height/Width}) \quad (1)$$

$$\text{Hausner ratio} = \text{Tapped density/Bulk density} \quad (2)$$

$$\text{Carr's index} = 100 \times (\text{Tapped density} - \text{Bulk density}) / (\text{Tapped density}) \quad (3)$$

2.4.2. Differential scanning calorimetry (DSC)

DSC measurements were performed with the aid of a DSC-60 Plus standard model, Shimadzu Corporation (Kyoto, Kyoto Prefecture, Japan). Samples of 2 mg of pure CRV and CRV-LSCs were encapsulated in hermetically sealed aluminum pans and heated from 20 °C to 200 °C at a scanning rate of 10 °C/min under a nitrogen purge of 40 ml/min.

2.4.3. Powder X-ray diffraction (PXRD)

The PXRD patterns of pure CRV and CRV-LSCs were obtained using Ultima IV diffractometer (Rigaku Inc., JAPAN). Samples were scanned over the 3–60° with diffraction angle 2θ range at a scan speed of 0.5 deg./min and collected pattern at 40 kV of tube voltage.

2.4.4. Fourier transform infrared (FT-IR) spectrometry

The possible interactions of CRV and tablet excipients used in the LSCs were studied using FTIR spectra that were obtained from a Nicolet iS10, Thermo Scientific Inc., (Waltham, MA, USA). Wavelength range was 4000 to 500 cm⁻¹ (resolution of 2 cm⁻¹).

2.5. Box-Behnken design for the optimization of CRV liquisolid formulations

Box Behnken design was employed to evaluate the effect of the solvent type (X₁), liquid load factor (X₂), and pH of the dissolution medium (X₃) on CRV dissolution from LSCs. The solvents used were chosen based on the solubility studies results (PEG 200, Tween 20, and PVP/VA 73). PEG 200 was coded as 1 and PVP/VA 73 was coded as 3 as they showed the lowest and the highest CRV solubilization efficiency, respectively, while Tween 20 was coded as 2 as it stands for the midpoint level of the three solvents used in the study. The liquid load factor was studied in the range of 0.15-0.25, while dissolution medium pH was studied in the range of 1.2 to 6.8. Statistical analysis was performed using Centurion XV Statgraphics®, Software (USA) to assess the effect of the independent variables on the crushing strength (Y₁), the disintegration time (Y₂), the dissolution rate in the first 10 minutes (Y₃), and the dissolution efficiency percent (Y₄). The composition of the optimized LSCs with improved dissolution pattern was obtained utilizing numerical optimization and desirability approach.

2.6. Preparation of CRV-LSCs

CRV-LSCs LS-1 to LS-15 were prepared. CRV was dispersed in the selected nonvolatile solvents. Avicel powder (carrier), and silica powder (coating) were then added to the dispersion with continuous mixing. Methocel (binder), Explotab (superdisintegrant), and magnesium trisilicate (adsorbent) are de-lumped individually through No. 40 mesh sieve. The de-lumped powders are mixed with the previous mixture for 15 min. Talc powder and magnesium stearate were also de-lumped through the 40-mesh sieve and then added to the powder blend and mixed for 3 min. The LSCs are made at 10 KN compression force in a single punch tablet press (Erweka, GmbH, Heusenstamm, Germany) equipped with 9 mm flat round tooling sets.

2.7. Evaluation of the prepared LSCs

The prepared tablets were evaluated for weight variation, content uniformity, friability, hardness and in vitro disintegration time according to the USP XXVIII [32]. The hardness of the

LSCs was presented in the design as the specific crushing strength of a tablet that is the ratio of LSCs hardness to LSCs' weight [33].

2.8. In vitro dissolution studies

In vitro dissolution studies were carried out using dissolution apparatus II (paddle type). 500 ml of the dissolution medium with different pH values (1.2, 4.0, and 6.8) at 37 °C were used at a rotation of 75 rpm. Samples (5 ml) were withdrawn at specified time intervals and filtered through 0.45 µm Millipore filter (Millipore Corp., Bedford, MA, USA). The concentration of CRV was determined spectrophotometrically at 242.5 nm using UV–Vis spectrophotometer (Jenway 7315, Bibby scientific Limited, Stone, Staffordshire, UK).

To investigate the significance of variation among the dissolution profiles of CRV from the prepared LSCs in comparison with the prepared conventional direct compressed tablet, the dissolution rate during the first 10 minutes (DR_{10}) and the dissolution efficiency at 60 min ($DE_{60}\%$) were computed according to the following equations [34–36]

$$DR_{10} = (M \times D) / 1000 \quad (4)$$

where M is the total quantity of CRV in each tablet (6250 µg) and D designates the percentage of drug dissolved during the first 10 min expressed as a decimal.

$$DE_{60} (\%) = \frac{\int_0^t Q dt}{Q_{100} \times t} \times 100 \quad (5)$$

where (Q) is the percent of drug released at each time interval, (t) is the total duration of drug release, and (Q100) is the 100% drug release.

2.9. Data analysis by BBD and prediction of the optimized CRV-LSCs formulation

The data of tablets specific crushing strength (Y_1), disintegration time (Y_2), dissolution rate in the first 10 min (Y_3), and dissolution efficiency at 60 min (Y_4) were statistically analyzed using Statgraphics software. The significance of the analysis was set for any factor at $p < 0.05$. The predicted optimized CRV-LSC formulation was prepared, evaluated and data obtained were compared with the predicted ones for residual calculations.

2.10. Dissolution profile comparison using similarity factor (f_2)

The similarity factor (f_2) was computed to compare the release profiles of the optimized LSCs and the conventional tablets using the following equation [37–39]

$$f_2 = 50 \log \left\{ \left[1 + \frac{1}{n} \sum_{t=1}^n W_t (R_t - T_t)^2 \right]^{-0.5} \times 100 \right\} \quad (6)$$

where, n is the number of time intervals at which % dissolved was determined, R_t and T_t represent the percentage drug dissolved of the two formulations to be compared at a given time interval. f_2 represents a logarithmic transformation of the sum of squared error of differences between the two formulations at all time intervals.

3. Results and discussion

Liquisolid is one of the formulation strategies to improve the solubility of poorly soluble drugs especially BCS class II. In this study, CRV was used as a model of this category.

3.1. Solubility studies

Following the saturated solubility study, it was apparent that CRV has very low solubility in water and the solubility substantially increased in the following vehicles in an ascending order: Glycerin, PG, PVP/VA 64, Span 80, PEG 400, PEG 200, Tween 20, and PVP/VA 73 as shown in

Figure 1. The three solvents with the highest solubilizing capacity for CRV were selected to be the liquid vehicles for preparing CRV liquisolid powder blends as this leads to enhanced release profiles [29,40,41]. In addition, the selection of a liquid vehicle with optimum solubilizing properties reduces the amount of liquid used leading to a decrease in the weight and size of the LSCs that represent a challenge in the formulation of LSCs.

3.2. Holding capacity and flowability parameters of the liquisolid excipients

To determine the maximum amount of a non-volatile liquid that can be held inside the bulk of the carrier and coating powders while maintaining an acceptable flowability, the optimum liquid load factor (L_f) was calculated. Table 1 revealed that the flowability parameters including the angle of repose, Hausner ratio, and Carr's index were remarkably improved upon decreasing the L_f of the powder blends. It was also clear from the results that the addition of silica improved the powder flow along with the studied range of L_f . This improvement could attribute to the high adsorptive property and large surface area of silica that gives the liquisolid system the desirable flow characteristics [42]. Regarding Carr's index, trials 4 and 5 had values less than 21% that indicates good flowability. Also, the results of the angle of repose confirmed the improvement of powder blends flowability upon the addition of silica. These results were considered a useful guide in the selection of L_f range that could be implemented in the response surface methodology as a factor to investigate its effect on the desired dissolution profile which must be met by the LSCs.

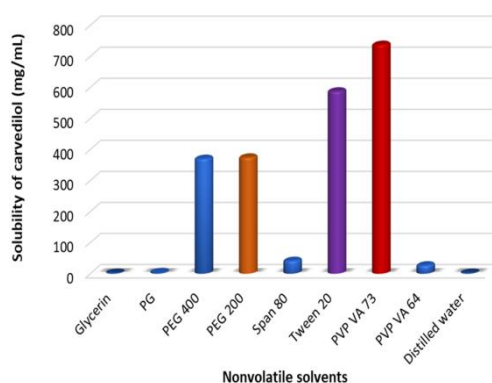


Fig. 1. Solubility of CRV in different nonvolatile solvents.

Table 1. Holding capacity and flowability parameters of the liquisolid excipients.

| Trial No. | $(L_f = W/Q)$ | Before the addition of silica | | | After the addition of silica | | |
|-----------|---------------|--------------------------------|---------------|------------------|--------------------------------|---------------|------------------|
| | | Angle of repose ($^{\circ}$) | Hausner ratio | Carr's index (%) | Angle of repose ($^{\circ}$) | Hausner ratio | Carr's index (%) |
| 1 | 0.5 | 41.5 | 1.59 | 37.37 | 38.54 | 1.57 | 36.61 |
| 2 | 0.4 | 40.24 | 1.49 | 32.55 | 37.75 | 1.44 | 30.43 |
| 3 | 0.3 | 38.98 | 1.38 | 27.74 | 36.97 | 1.32 | 24.25 |
| 4 | 0.2 | 31.68 | 1.24 | 18.28 | 29.83 | 1.14 | 15.19 |
| 5 | 0.1 | 30.69 | 1.16 | 14.13 | 24.38 | 1.09 | 8.82 |

3.3. Pre-compression evaluation of CRV liquisolid formulations

The composition of the CRV-LSC formulations as suggested by Box-Behnken design was presented in Table 2. The powder blend of all formulations was evaluated before and after compression.

3.3.1. Evaluation of flow and packing properties

The micromeritic properties of the pre-compressed liquisolid powder blends such as Hausner's ratio, Carr's index, and angle of repose were found to be in the range of 1.09-1.32, 6.06-24.43, and 19-41°, respectively which indicate that the pre-compressed powder blends for all formulations showing acceptable flow properties. It was obvious from the data in Table 3 that most of LS formulations containing Tween 20 as a liquid medication (LS-5, LS-11, LS-14, and LS-15) had passable flow. These formulations showed the highest values of Hausner ratio, Carr's index, and angle of repose. On the other hand, formulations containing PEG 200 exhibited good flowability as the value of Hausner ratio was less than 1.2 [43]. Also, these formulations showed good flowability and can be compressed as Carr's index data showed results of less than 21 %.[44] Finally, it was found that formulations that contain very viscous liquid vehicles such as PVP/VA 73 revealed excellent flowability with the lowest values of Hausner ratio, Carr's index, and angle of repose [42,45]. This enhanced flowability and compressibility of the PVP/VA 73 containing formulations reflected in increased tablet's hardness values, retarded disintegration time, and controlled CRV release.

Table 2. Composition of carvedilol Liquisolid formulations based on Box-Behnken design.

| Run # | Avicel, Q | Silica, q | Liquid medication, W | | | CRV | Methocel | Mg trisilicate | Explotab | Talc | Mg stearate | Tablet weight |
|--------|--------------|--------------|----------------------|-------------|---------------|------|----------|-------------------|----------|------|----------------|------------------|
| | | | PEG 200 | Tween 20 | PVP/ VA 73 | | | | | | | |
| | (mg) | | | | | | | | | | | |
| LS -1 | 166.67 | 8.33 | 41.67 | --- | --- | 6.25 | 13.38 | 11.15 | 13.38 | 2.61 | 2.61 | 266.03 |
| LS -2 | 166.67 | 8.33 | 25.00 | --- | --- | 6.25 | 12.38 | 10.31 | 12.38 | 2.41 | 2.41 | 246.14 |
| LS -3 | 166.67 | 8.33 | --- | 25.00 | --- | 6.25 | 12.38 | 10.31 | 12.38 | 2.41 | 2.41 | 246.14 |
| LS -4 | 166.67 | 8.33 | --- | --- | 33.33 | 6.25 | 12.88 | 10.73 | 12.88 | 2.51 | 2.51 | 256.08 |
| LS -5 | 166.67 | 8.33 | --- | 41.67 | --- | 6.25 | 13.38 | 11.15 | 13.38 | 2.61 | 2.61 | 266.03 |
| LS -6 | 166.67 | 8.33 | --- | --- | 25.00 | 6.25 | 12.38 | 10.31 | 12.38 | 2.41 | 2.41 | 246.14 |
| LS -7 | 166.67 | 8.33 | --- | 25.00 | --- | 6.25 | 12.38 | 10.31 | 12.38 | 2.41 | 2.41 | 246.14 |
| LS -8 | 166.67 | 8.33 | 33.33 | --- | --- | 6.25 | 12.88 | 10.73 | 12.88 | 2.51 | 2.51 | 256.08 |
| LS -9 | 166.67 | 8.33 | --- | --- | 41.67 | 6.25 | 13.38 | 11.15 | 13.38 | 2.61 | 2.61 | 266.03 |
| LS -10 | 166.67 | 8.33 | --- | --- | 33.33 | 6.25 | 12.88 | 10.73 | 12.88 | 2.51 | 2.51 | 256.08 |
| LS -11 | 166.67 | 8.33 | --- | 41.67 | --- | 6.25 | 13.38 | 11.15 | 13.38 | 2.61 | 2.61 | 266.03 |
| LS -12 | 166.67 | 8.33 | 33.33 | --- | --- | 6.25 | 12.88 | 10.73 | 12.88 | 2.51 | 2.51 | 256.08 |
| LS -13 | 166.67 | 8.33 | --- | 33.33 | --- | 6.25 | 12.88 | 10.73 | 12.88 | 2.51 | 2.51 | 256.08 |
| LS -14 | 166.67 | 8.33 | --- | 33.33 | --- | 6.25 | 12.88 | 10.73 | 12.88 | 2.51 | 2.51 | 256.08 |
| LS -15 | 166.67 | 8.33 | --- | 33.33 | --- | 6.25 | 12.88 | 10.73 | 12.88 | 2.51 | 2.51 | 256.08 |

Table 3. Pre-compression and post-compression properties of carvedilol liquisolid formulations.

| Run # | Hausner ratio | Carr's index (%) | Angle of repose (°) | Type of flow | Weight (mg) | Content Uniformity (%) | Hardness (N) | Friability (%) |
|--------|---------------|------------------|---------------------|--------------|-------------|------------------------|--------------|----------------|
| LS -1 | 1.17 | 14.81 | 34 | Good | 265 | 99.35 | 62.43 | 0.53 |
| LS -2 | 1.12 | 10.79 | 31 | Good | 244 | 98.73 | 76.05 | 0.46 |
| LS -3 | 1.21 | 17.33 | 35 | Fair | 243 | 96.98 | 59.09 | 0.57 |
| LS -4 | 1.07 | 6.72 | 21 | Excellent | 254 | 97.33 | 258.03 | 0.12 |
| LS -5 | 1.31 | 23.61 | 42 | Passable | 263 | 97.29 | 44.88 | 0.73 |
| LS -6 | 1.09 | 8.61 | 23 | Excellent | 242 | 98.73 | 196.98 | 0.27 |
| LS -7 | 1.23 | 18.62 | 36 | Fair | 241 | 95.35 | 65.66 | 0.53 |
| LS -8 | 1.14 | 11.99 | 32 | Good | 252 | 97.73 | 66.93 | 0.76 |
| LS -9 | 1.10 | 9.45 | 25 | Excellent | 261 | 96.18 | 181.59 | 0.28 |
| LS -10 | 1.06 | 6.06 | 19 | Excellent | 253 | 97.33 | 229.42 | 0.23 |
| LS -11 | 1.32 | 24.43 | 43 | Passable | 266 | 96.29 | 41.55 | 0.76 |
| LS -12 | 1.12 | 10.81 | 31 | Good | 255 | 97.73 | 61.05 | 0.72 |
| LS -13 | 1.24 | 19.27 | 37 | Fair | 252 | 99.29 | 54.49 | 0.57 |
| LS -14 | 1.28 | 22.01 | 41 | Passable | 253 | 98.73 | 56.64 | 0.63 |
| LS -15 | 1.29 | 22.95 | 41 | Passable | 253 | 99.35 | 53.80 | 0.51 |

3.3.2. Differential scanning calorimetry (DSC)

DSC thermograms of pure CRV and CRV liquisolid powder blend are shown in Figure 2a. CRV pure showed a sharp endothermic peak at melting temperature (115.61 °C) with relatively high enthalpy value (-219.23 mJ/g). This sharp peak indicates CRV crystallinity and melting of the sample, referring to the end of the thermogram to the decomposition of CRV. The thermogram of LS formulation showed a very small peak at 116.55 °C with a very small enthalpy value of -8.48 mJ/g. Moreover, the disappearance of the sharp endothermic peak in the LS formulation indicates the change of CRV from the crystalline to the amorphous state. This result could also refer to a possibility of interaction as H-bond formation between the vehicle and CRV as reported in the literature [15,46,47].

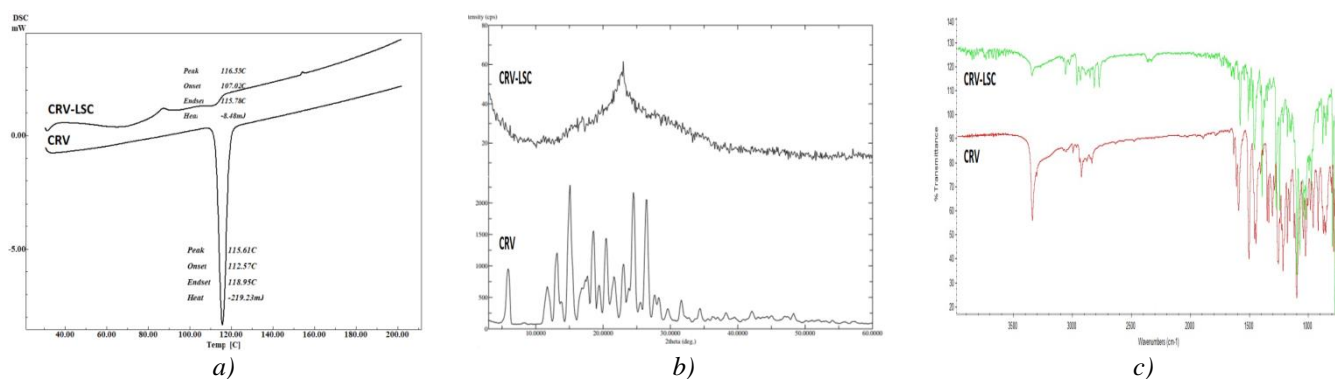


Fig. 2. DSC thermograms (a), Powder X-ray diffractograms (b), and FT-IR spectra (b) of pure carvedilol powder and carvedilol liquisolid compacts.

3.3.3. Powder X-ray diffraction (PXRD)

Characterization using an X-ray diffractometer showed differences between the diffractogram of pure CRV, and powder blend of the liquisolid formulation (Figure 2b). The crystallinity peaks of CRV are clearly showed at 2θ of 5.72; 11.53; 12.87; 14.72; 16.36; 17.43; 18.36; 24.13; 26.07; and 29.30. While the diffractogram of LS powder blend showed disappearance of CRV distinct peaks with a reduction in the height of those peaks with an increase in their width that indicated CRV amorphous form. The molecularly dissolved state of CRV in the non-volatile solvent used in the formulation created CRV amorphous form. The change of CRV molecular dispersion to amorphous form enhances the dissolution rate and solubility of CRV [48,49].

3.3.4. FTIR spectroscopy

To investigate the potential interactions of CRV and the utilized excipients in the LSC, FTIR spectra interpretation was presented in Figure 2c. CRV show peaks at 3,330-3,000 cm^{-1} for hydrogen bonding of N-H and O-H; 3,050-2,950 cm^{-1} for C-H (vibration aliphatic and/or aromatic); 1,650 for N-H bending; 1,600 and 1,500 cm^{-1} for C=C aromatic vibration.[50] From Figure 2c, the FTIR spectra provide information about the pure CRV and the LS formulation. The fingerprint CRV peaks in the region 3,500 cm^{-1} to 2,800 cm^{-1} showed marked changes in the spectrum when compared with the LS formulation. These include reduced in the intensity of the signal that could indicate the interaction between CRV and LSC excipients. There is hydrogen bonding between N-H and/or O-H functional groups in CRV with any hydrogen bond acceptor groups of LSC excipients. Hydrogen bonds formation between CRV and the LSC vehicle improves CRV solubility, that reflects on its dissolution profiles. The FTIR data were in line with DSC and PXRD findings, which revealed the solubilization of CRV crystals in the liquid vehicles, reducing CRV crystallinity.

3.4. Post-compression evaluation of CRV liquisolid formulations

Quality control tests of the prepared CRV-LSCs presented in Table 3 revealed that the content uniformity of all formulations was found to be in the range of 95.35 % (LS-7) to 99.35 % (LS-1 and LS-15). These results were complied with the official specifications of USP and reflect the uniformity of weight in all formulations [51]. Also, there is no variation in the thickness of all formulations. The friability and the hardness of all LSCs ranged from 0.12-0.76 %, and 41.55-258.03 N, respectively. The friability and hardness results reflected the acceptable mechanical properties and good breaking strength of the prepared CRV-LSCs as well as overcome the poor compressibility of the liquisolid powders [52]. Finally, it was noticed that the type of non-volatile solvent affected remarkably on the hardness and subsequently on tablet disintegration. This finding displayed from formulations containing PVP/VA 73 (LS-4, LS-6, LS-9, and LS-10) that showed the highest hardness values and the longest disintegration time. Accordingly, despite the highest solubilizing capacity of PVP/VA for CRV, PVP/VA is not recommended to be used in immediate-release formulations and could be of great value in controlling the release of drugs due to its excellent property as a dry binder for direct compression process.

3.5. Response surface methodology for optimization of CRV-LSCs

Box Behnken design was utilized for the optimization of CRV-LSCs with acceptable crushing strength, minimized disintegration time and enhanced drug dissolution via different parameters. The experimental matrix and the measured responses are compiled in Table 4.

3.5.1. Influence of independent variables on tablet crushing strength (Y_1)

Crushing strength is a crucial test for evaluating the mechanical durability of LSCs. Table 4 showed that the prepared LSCs have a marked variation in the crushing strength ranging from 15.94 kg/g (LS-11) to 103.66 kg/g (LS-4). The quadratic model exhibited a high correlation coefficient and adjusted correlation coefficient indicating model fitting of the data (Table 5). The polynomial equation was generated as follows:

$$\begin{aligned} \text{Specific crushing strength} \\ (Y_1, \text{kg/g}) = & -71.4594 + 5.98702 X_1 + 532.317 X_2 + 14.9397 X_3 + 17.3708 X_1^2 - 357.4 X_1 X_2 \\ & + 2.28929 X_1 X_3 + 1088.33 X_2^2 - 128.25 X_2 X_3 + 1.85597 X_3^2 \end{aligned} \quad (7)$$

Analysis of variance (ANOVA) revealed a significant positive effect for both the linear (X_1) and the quadratic terms (X_1^2) of solvent type on the tablets' crushing strength with p-values of 0.0305 and 0.0437, respectively as shown in Table 5 and in Pareto chart (Figure 3a). It was evident that formulations prepared using PVP/VA 73 as a solvent showed the highest crushing strength as demonstrated in the three-dimensional surface plots for the effect of the investigated factors on the crushing strength (Fig. 3 b & d). This effect could be attributed to the binding action of the liquid vehicle in low concentrations owing to the possible formation of hydrogen bonds between the solvent and other excipients in LS formulations with consequent mechanical interlocking [25]. On the other hand, the liquid load factor (X_2) was inversely proportional to the crushing strength of the tablets. Table 5, Pareto chart (Fig. 3a), and the 3D response surface plots (Fig. 3 b & c) revealed a significant negative effect of X_2 on Y_1 with a p-value of 0.0317. When the Lf increased from 0.15 (LS-2) to 0.25 (LS-1) in PEG 200 based formulations, the crushing strength of the tablets decreased from 31.0 to 24.04 kg/g. Also, in Tween 20 based formulations, the crushing strength of tablets decreased from 24.81 kg/g (LS-3) to 17.41 kg/g (LS-5) when Lf increased from 0.15 to 0.25. The same finding was observed with PVP/VA based formulations. This finding could be explained by the tensile strength of Avicel® compacts that continuously decrease with increasing liquid drug content due to its plastic deformation [53,54].

Table 4. Experimental matrix of CRV-LSTs as suggested by Box-Behnken design.

| Run # | Independent variables | | | Dependent variables | | | |
|-------|------------------------|------------------------------|------------------------------------|--------------------------------------|-------------------------------|----------------------------|----------------------------------|
| | Solvent type (X_1) | Liquid load factor (X_2) | pH of dissolution medium (X_3) | Specific crushing strength (Y_1) | Disintegration time (Y_2) | Dissolution rate (Y_3) | Dissolution efficiency (Y_4) |
| LS-1 | PEG 200 | 0.25 | 4.0 | 24.04 | 11.36 | 198.40 | 55.46 |
| LS-2 | PEG 200 | 0.15 | 4.0 | 31.80 | 21.55 | 148.74 | 53.73 |
| LS-3 | Tween 20 | 0.15 | 1.2 | 24.81 | 8.43 | 249.56 | 61.69 |
| LS-4 | PVP VA 73 | 0.20 | 1.2 | 103.66 | 121.5 | 9.09 | 8.91 |
| LS-5 | Tween 20 | 0.25 | 1.2 | 17.41 | 6.25 | 187.28 | 70.40 |
| LS-6 | PVP VA 73 | 0.15 | 4.0 | 83.06 | 118.0 | 44.07 | 10.86 |
| LS-7 | Tween 20 | 0.15 | 6.8 | 27.80 | 8.18 | 41.06 | 22.42 |
| LS-8 | PEG 200 | 0.20 | 6.8 | 27.10 | 16.21 | 5.80 | 8.58 |
| LS-9 | PVP VA 73 | 0.25 | 4.0 | 71.00 | 132.0 | 51.62 | 12.46 |
| LS-10 | PVP VA 73 | 0.20 | 6.8 | 92.53 | 136.0 | 16.91 | 3.95 |
| LS-11 | Tween 20 | 0.25 | 6.8 | 15.94 | 6.52 | 108.27 | 28.63 |
| LS-12 | PEG 200 | 0.20 | 1.2 | 24.43 | 18.54 | 163.42 | 52.30 |
| LS-13 | Tween 20 | 0.20 | 4.0 | 22.06 | 7.31 | 549.60 | 88.51 |
| LS-14 | Tween 20 | 0.20 | 4.0 | 22.85 | 7.51 | 549.60 | 88.52 |
| LS-15 | Tween 20 | 0.20 | 4.0 | 21.70 | 7.15 | 549.60 | 88.56 |

3.5.2. Influence of independent variables on tablet disintegration (Y_2)

Fast disintegration of tablets is necessary to ensure tablets' rapid break down into smaller fragments to yield the largest possible surface area accessible for dissolution media [55]. The prepared LSCs showed marked variations in disintegration times ranging from 6.25 min (LS-11) to 121.5 min (LS-4). The pattern of disintegration time was in accordance with the crushing strength, i.e. disintegration time increased with the increase in crushing strength (Table 4). Disintegration

time data fitted the quadratic model as evidenced by the high determined correlation and adjusted correlation coefficients (Table 5). The polynomial equation was generated as follows:

$$\begin{aligned} \text{In-vitro disintegration time} \\ (Y_2, \text{ min}) = & -181.565 + 23.021 X_1 + 1161.22 X_2 + 29.196 X_3 + 31.336 X_1^2 - 621.95 X_1 X_2 - 2.035 X_1 X_3 \\ & + 933.333 X_2^2 - 208.607 X_2 X_3 + 3.943 X_3^2 \end{aligned} \quad (8)$$

As depicted in Table 5 and Figure 4a, ANOVA showed a significant effect of the linear terms (X_3 and X_2) corresponding to the pH of the dissolution medium and the liquid load factor of the formulations with p-values of 0.0087 and 0.0421, respectively. PVP/VA based formulations showed the longest disintegration times as demonstrated in the 3D response surface plots for the effect of the investigated factors on the disintegration time (Figure 4 b-d). This effect could be credited to the highest crushing strength with possible consequent low porosity demonstrated by PVP/VA based formulations owing to the binding action and mechanical interlocking effect of the solvent [56]. A similar trend for the relation between crushing strength and disintegration time of spironolactone LSCs previously prepared by Elkordy et al [55]. However, in PVP/VA based formulations the disintegration time decreased by increasing the L_f of the formulation from 0.15 to 0.25 as shown in Figure 4b. Also, in Tween 20 based formulations the disintegration time was significantly influenced by pH especially at lower values of X_2 and this effect of pH decreased by increasing X_2 (Figure 4c). The effect of pH was depicted on LS formulations whatever the solvent used especially at the mid-point of L_f as displayed in Figure 4d.

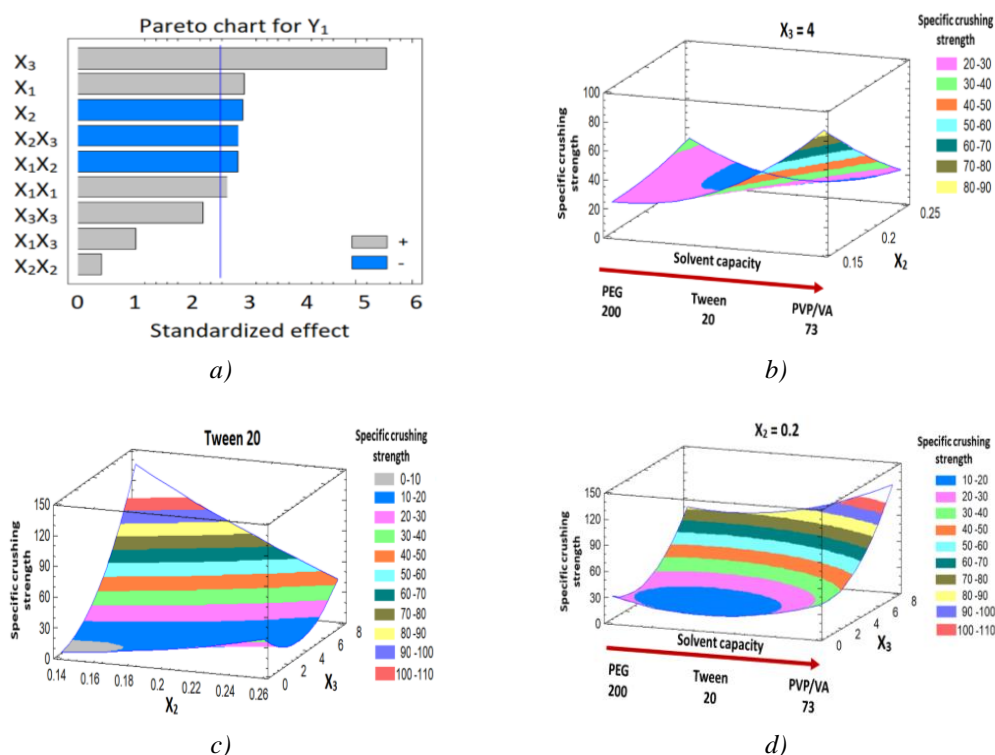


Fig. 3. Standardized Pareto chart (a) and 3D response surface plots (b-d) showing the effect of solvent capacity (X_1), liquid load factor (X_2), and pH of the dissolution medium (X_3) on the response Y_1 .

3.5.3. Influence of independent variables on dissolution parameters (Y_3 and Y_4)

Dissolution profiles of CRV-LSCs and directly compressed conventional tablets were depicted in Fig. 5. Results revealed the drug release from LSCs, whatever the solvent used in their preparation, is significantly faster than that from their corresponding directly compressed ones. It was evident that drug dissolution from directly compressed tablets (DCT) was slow and incomplete

within 60 min for all studied pH values. The highest amount obtained of CRV released from the DCT was only 20% after 1 h, however, a similar amount was released within 5 min from the corresponding LSCs. Dissolution enhancement of CRV from LSCs might be ascribed to the existence of the drug in a solubilized form in LSCs that increased its surface area available for dissolution, increased drug aqueous solubility, and improved drug's wettability by the dissolution medium [57–60]. Dissolution improvement could improve CRV absorption in the gastrointestinal tract and subsequently enhance its oral bioavailability [61].

To compare the dissolution profiles, both dissolution rate during the first 10 minutes (DR10, $\mu\text{g}/\text{min}$; Y_3) and dissolution efficiency after 60 min ($DE_{60}\%$, Y_4) were computed and compiled in Table 4. The high determined correlation and adjusted correlation coefficients indicate the fitting of the dissolution parameters into the quadratic model (Table 5). The polynomial equations of the terms of coded factors were generated as follow:

Dissolution rate

$$(Y_3, \mu\text{g}/\text{min}) = -3630.99 + 405.725 X_1 + 32796.3 X_2 + 262.583 X_3 - 198.493 X_1^2 + 1949.95 X_1 X_2 - 1.66696 X_1 X_3 - 89850.0 X_2^2 - 140.607 X_2 X_3 - 31.6652 X_3^2 \quad (9)$$

Dissolution efficiency

$$(Y_4, \%) = -398.721 - 16.048 X_1 + 4463.97 X_2 + 31.961 X_3 - 21.041 X_1^2 + 453.9 X_1 X_2 + 1.299 X_1 X_3 - 12643.5 X_2^2 - 48.893 X_2 X_3 - 4.014 X_3^2 \quad (10)$$

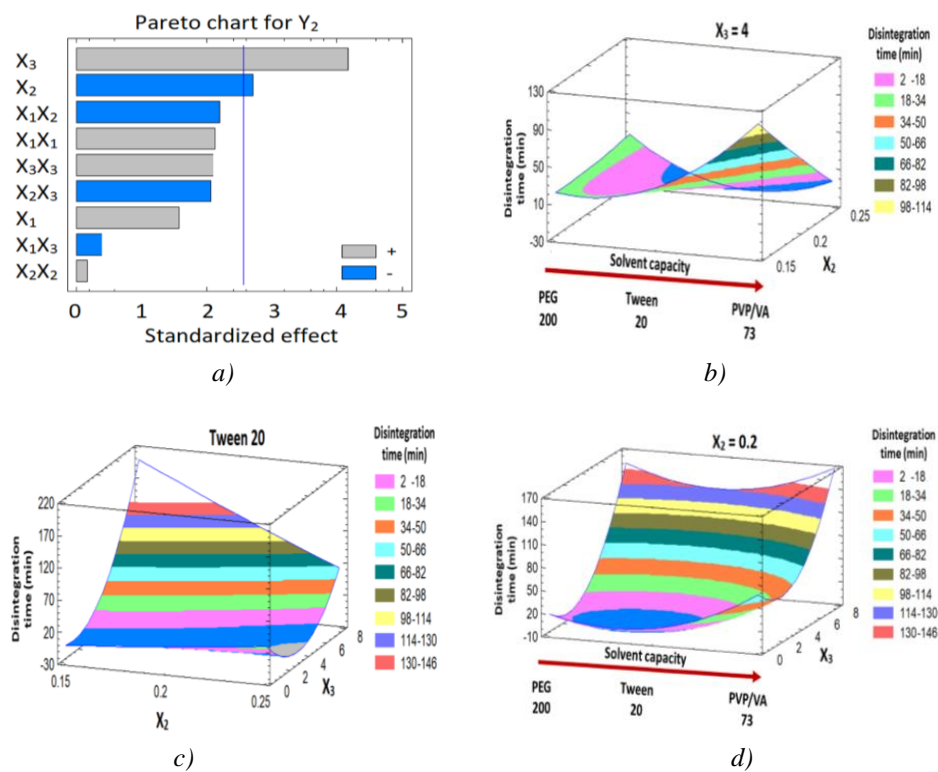


Fig. 4. Standardized Pareto chart (a) and 3D response surface plots (b-d) showing the effect of solvent capacity (X_1), liquid load factor (X_2), and pH of the dissolution medium (X_3) on the response Y_2 .

Table 5. Statistical analysis of variance (ANOVA) of the responses (Y_1 - Y_4) results.

| Factors | Specific crushing strength (Y_1) | | Disintegration time (Y_2), min | | Dissolution rate (Y_3), $\mu\text{g}/\text{min}$ | | Dissolution efficiency (Y_4), % | |
|------------|--------------------------------------|---------|------------------------------------|---------|--|---------|-------------------------------------|---------|
| | Estimate | P-Value | Estimate | P-Value | Estimate | P-Value | Estimate | P-Value |
| X_1 | 26.295 | 0.0305* | 31.67 | 0.1748 | -9.845 | 0.5694 | -8.4725 | 0.1138 |
| X_2 | -26.015 | 0.0317* | -54.3775 | 0.0421* | 19.3775 | 0.2846 | 11.88 | 0.0436* |
| X_3 | 48.81 | 0.0026* | 83.7125 | 0.0087* | -124.283 | 0.0006* | -41.0625 | 0.0002* |
| X_1X_1 | 34.7417 | 0.0437* | 62.6717 | 0.0869 | -396.985 | 0.0000* | -42.0825 | 0.0013* |
| X_1X_2 | -35.74 | 0.0349* | -62.195 | 0.0796 | 194.995 | 0.0004* | 45.39 | 0.0008* |
| X_1X_3 | 12.82 | 0.3503 | -11.395 | 0.7042 | -9.335 | 0.7001 | 7.275 | 0.2976 |
| X_2X_2 | 5.44167 | 0.6919 | 4.66667 | 0.8805 | -449.25 | 0.0000* | -63.2175 | 0.0002* |
| X_2X_3 | -35.91 | 0.0344* | -58.41 | 0.0943 | -39.37 | 0.1459 | -13.69 | 0.0804 |
| X_3X_3 | 29.1017 | 0.0746 | 61.8267 | 0.0902 | -496.51 | 0.0000* | -62.9425 | 0.0002* |
| R^2 | 93.9337 | | 89.9696 | | 99.5326 | | 98.6141 | |
| Adj. R^2 | 83.0143 | | 71.9148 | | 98.6914 | | 96.1193 | |

Note: *Significant effect of factors on individual responses.

Abbreviations: X_1 , Solvent type; X_2 , Liquid load factor; X_3 , pH of dissolution medium; X_1X_2 , X_1X_3 , X_2X_3 , the interaction term between the factors; X_1X_1 , X_2X_2 , and X_3X_3 are the quadratic terms between the factors; R^2 , R-squared; Adj- R^2 , Adjusted R-squared; SEE, standard error of estimate; and MAE, Mean absolute error.

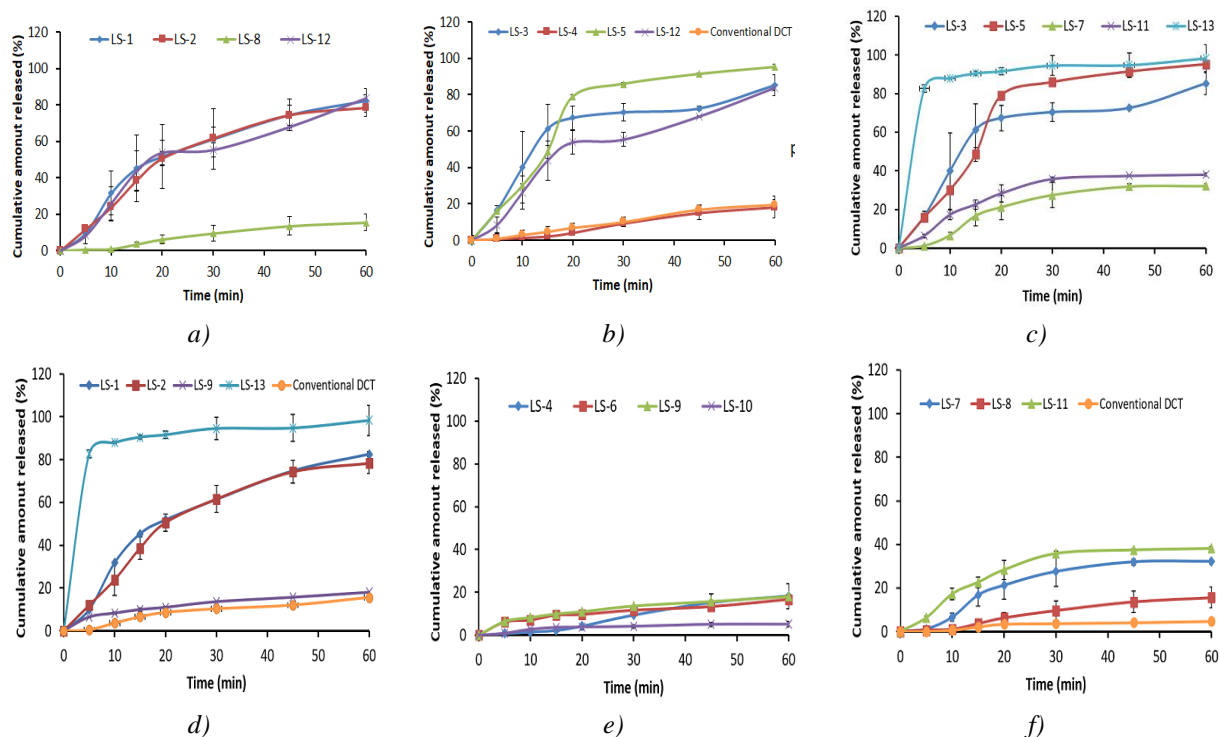


Fig. 5. Dissolution profiles of the prepared carvedilol liquisolid formulations in different pH compared with the conventional direct compressed tablets.

a) PEG 200, b) pH 1.2, c) Tween 20, d) pH 4.0, e) PVP/VA 73, pH 6.8.

Statistical analysis showed a significant negative effect of the quadratic terms for all the studied factors and the linear term X_3 (pH of the dissolution medium). On the other hand, the interaction term of X_1 and X_2 showed a significant positive effect on both dissolution rate and efficiency at a 95% level of significance as demonstrated in the Pareto charts presented in Figures 6a and 7a. On the other hand, the linear term of X_2 (liquid load factor) displayed a significant positive effect on the dissolution efficiency (Y_4). The effects of the studied factors and the interaction between them on dissolution rate and efficiency are graphically illustrated in the three-dimensional surface plots shown in Figures 6b-d and 7b-d, respectively.

It was evident that liquisolid formulations prepared using Tween 20 exhibited the highest dissolution followed by those prepared using PEG 200. The lowest dissolution rates and efficiency were observed in formulation prepared using PVP/VA 73 although the drug showed the highest solubility in this solvent. This could be attributed to PVP/VA 73 ability for preserving CRV molecules that in good accordance with the results observed by Adibkia et al [62].

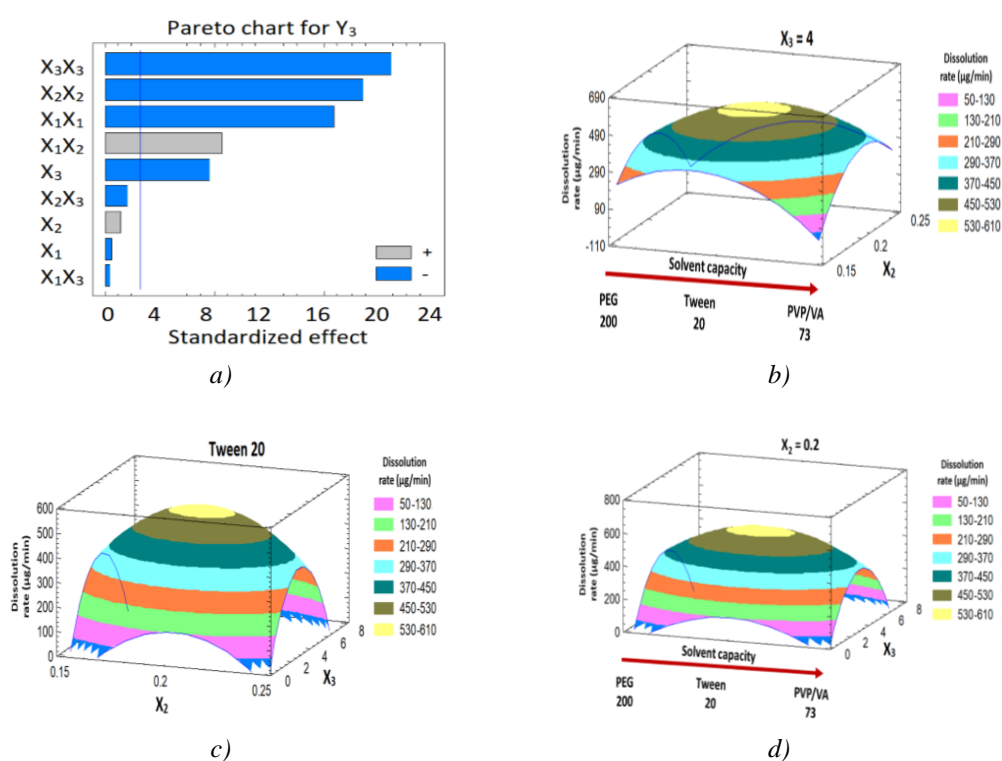


Fig. 6. Standardized Pareto chart (a) and 3D response surface plots (b-d) showing the effect of solvent capacity (X_1), liquid load factor (X_2), and pH of the dissolution medium (X_3) on the response Y_3 .

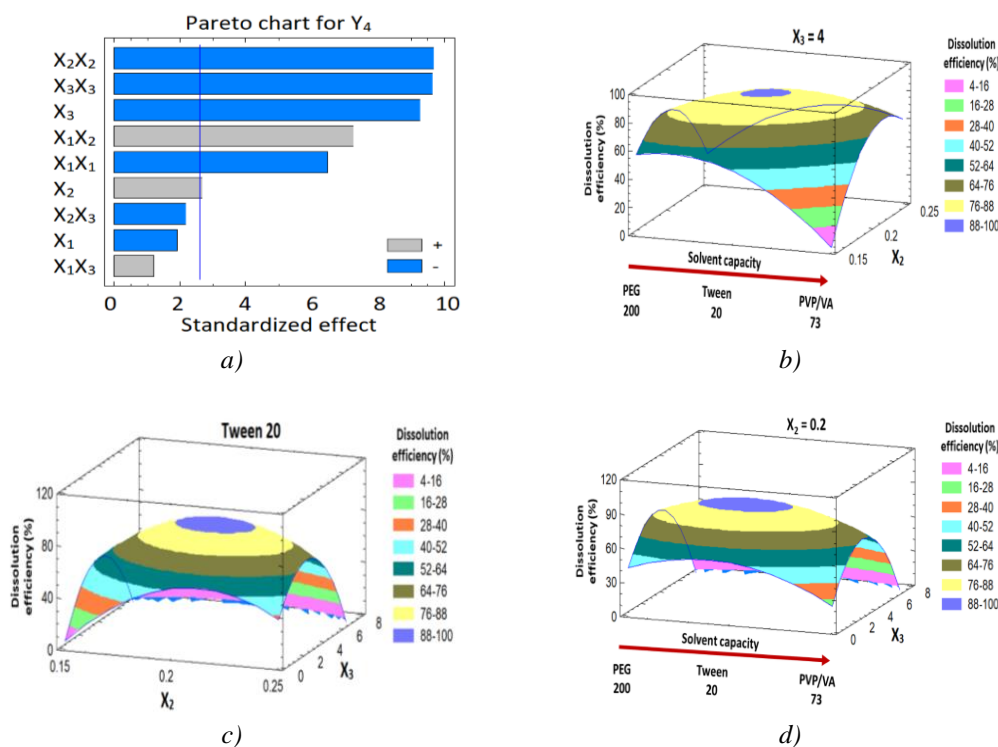


Fig. 7. Standardized Pareto chart (a) and 3D response surface plots (b-d) showing the effect of solvent capacity (X_1), liquid load factor (X_2), and pH of the dissolution medium (X_3) on the response Y_4 .

Regarding the effect of dissolution medium pH on CRV release, the highest release was achieved at pH 4 followed by pH 1.2, while the lowest results were observed at pH 6.8. CRV has \square -hydroxyl group of the secondary amine (pKa 7.8) and shows pH-dependent solubility. The drug solubility improves with the increase in pH and then the solubility starts to decline after pH 4. The solubility of CRV at lower pH values is determined by its protonated form and its in-situ formed salt. The hydrochloride salt formed in-situ in low pH medium might have lower solubility than the protonated CRV in this medium [6]. This pattern was observed for both DCT and LSCs. However, a prominent enhancement in drug dissolution was observed for LSCs in comparison to DCT at the three studied pH values that could be explained by the ability of LSCs to present CRV in a fine molecularly dispersed state upon disintegration as previously mentioned.

3.5.4. Optimization

Numerical optimization following the desirability function approach was applied to predict the optimum LSCs composition with acceptable crushing strength, minimized disintegration time and enhanced CRV dissolution. The optimized formulation was generated at X_1 , X_2 and X_3 levels of Tween 20 (solvent type), 0.198 (liquid load factor), and 4.0 (pH of dissolution medium). The optimized formulation fulfilled the requirements with the desirability of 0.956. The optimized LSCs exhibited specific crushing strength of 30 kg/g, disintegration time of 18 min, the dissolution rate of 524.68 $\mu\text{g}/\text{min}$, and dissolution efficiency of 83.58%. The observed parameters were in good agreement with the predicted ones with a percentage error of less than 5%.

Finally, the dissolution profile of the optimized formulation was compared with that of the DCT at pH 4 according to the similarity factor approach [63]. For dissolution profiles to be considered similar, the value of similarity factor (f_2) should be as close as possible to 100 (range from 50 to 100, where f_2 values of 50 and 100 correspond to 10% and 0% differences, respectively). The computed f_2 value was 8.23 (i.e. <50) indicating the dissolution profile of LSCs differs significantly from DCTs.

4. Conclusions

From the obtained results, it was found that PVP/VA has the highest solubility of CRV among the other solvents. The flowability of the liquisolid powder blend showed acceptable results with the addition of solvent and further improved with the addition of silica, which would be suitable for the preparation of LSCs. The type of non-volatile solvent affects remarkably the hardness and subsequently the disintegration of the LSCs.

Formulations contain PVP/VA showed the highest hardness values and the longest disintegration time which in turn is not recommended to be used in immediate-release formulations and could be of great value in controlling drug release. On the other hand, Tween 20 displayed excellent behavior as a non-volatile solvent in the preparation of LSCs designed for rapid drug release due to its activity as solubilizing and wetting agents. Finally, the liquisolid technique enhanced the dissolution profile of poorly soluble drugs and can be utilized as an alternative tool in the production of immediate-release formulations.

Acknowledgments

This project was funded by the Deanship of Scientific Research (DSR) at King Abdulaziz University, Jeddah, under grant no. G-141-166-38. The authors, therefore, acknowledge with thanks DSR for technical and financial support.

References

- [1] H. Wen, H. Jiang, Z. Lu, X. Hu, B. He, Q. Tang, C. Huang, *Biomed. Pharmacother.* **64**, 446 (2010).
- [2] S. Chakraborty, D. Shukla, A. Jain, B. Mishra, S. Singh, *J. Colloid Interface Sci.* **335**, 242 (2009).
- [3] T. Morgan, *Clin. Pharmacokinet.* **26**, 335 (1994).
- [4] B. Singh, R. Singh, S. Bandyopadhyay, R. Kapil, B. Garg, *Colloids Surf. B. Biointerfaces* **101**, 465 (2013).
- [5] X. Wen, F. Tan, Z. Jing, *Z. J. Pharm. Biomed. Anal.* **34**, 517 (2004).
- [6] B. D. Shewale, N. P. Sapkal, N. A. Raut, N. J. Gaikwad, R. A. Fursule, *Indian J. Pharm. Sci.* **70**, 255 (2008).
- [7] O. Planinšek, B. Kovačič, F. Vrečer, *Int. J. Pharm.* **406**, 41 (2011).
- [8] V. K. Venishetty, R. Chede, R. Komuravelli, L. Adepu, R. Sistla, P. V. Diwan, *Colloids Surf. B. Biointerfaces* **95**, 1 (2012).
- [9] K. M. Hosny, K. M. El-Say, H. M. Alkhalidi, *J. Drug Deliv. Sci. Technol.* **45**, 168 (2018).
- [10] K. M. El-Say, K. M. Hosny, *PLoS One* **13**, e0203405 (2018).
- [11] S. Patil, A. Babbar, R. Mathur, A. Mishra, K. Sawant, *J. Drug Target.* **18**, 321 (2010).
- [12] U. Ubaidulla, M. V. S. Reddy, K. Ruckmani, F. J. Ahmad, R. K. Khar, *AAPS PharmSciTech* **8**, E1 (2007).
- [13] A. A. Aboelwafa, D. A. El-Setouhy, A. N. Elmeshad, *AAPS PharmSciTech* **11**, 1591 (2010).
- [14] A. Kaur, G. Kaur, *Saudi Pharm. J.* **20**, 21 (2012).
- [15] Y. H. M. Aljimaee, A. M. El-Helw, O. A. A. Ahmed, K. M. El-Say, *Drug Des. Devel. Ther.* **9**, 1379 (2015).
- [16] M. Harikrishna, R. Akki, M. G. Ramya, P. V. A. Neelima, V. V. Naik, *Der Pharm. Lett.* **6**, 403 (2014).
- [17] D. Hasanthi, J. N. S. Kumar, N. Guntur, A. Pradesh, *Int. J. Res. Pharm. Nano Sci.* **1**, 170 (2012).
- [18] V. S. Meka, V. H. W. Liang, S. R. Dharmalingham, R. Sheshala, A. Gorajana, *Acta Pharm.* **64**, 485 (2014).
- [19] M. Yelugam, K. B. Koteswara, R. M. Sreenivasa, *Int. J. Pharm. Pharm. Sci.* **5**, 686 (2013).
- [20] M. V. Nila, M. R. Sudhir, T. A. Cinu, N. A. Aleykutty, S. Jose, *Drug Deliv.* **21**, 110 (2014).
- [21] R. Fahmy, M. Kassem, *Eur. J. Pharm. Biopharm.* **69**, 993 (2008).
- [22] B. Vraníková, J. Gajdziok, *Acta Pharm.* **63**, 447 (2013).

- [23] S. A. Tayel, I. I. Soliman, D. Louis, *Eur J Pharm Biopharm* **69**, 342 (2008).
- [24] K. M. El-Say, A. M. Samy, M. I. Fetouh, *J. Pharm. Res.* **3**, 2388 (2010).
- [25] Y. Javadzadeh, B. Jafari-Navimipour, A. Nokhodchi, *Int. J. Pharm.* **341**, 26 (2007).
- [26] N. Tiong, A. A. Elkordy, *Eur. J. Pharm. Biopharm.* **73**, 373 (2009).
- [27] P. Walke, A. Pawar, D. Sonawane, R. Bhamber, *J. Pharm. Res.* **4**, 4011 (2011).
- [28] M. Saeedi, J. Akbari, K. Morteza-Semnani, R. Enayati-Fard, S. Sar-Reshteh-Dar, A. Soleymani, *Iran. J. Pharm. Res.* **10**, 25 (2011).
- [29] A. Nokhodchi, Y. Javadzadeh, M. R. Siahi-Shadbad, M. Barzegar-Jalali, *J. Pharm. Pharm. Sci.* **8**, 18 (2005).
- [30] D. R. Komala, K. Y. Janga, R. Jukanti, S. Bandari, M. Vijayagopal, *J. Drug Deliv. Sci. Technol.* **30**, 232 (2015).
- [31] A. Martin, P. Bustamante, A. H. C. Chun, "Physical Pharmacy; Physical Chemical Principles in the Pharmaceutical Sciences", Lippincott Williams&Wilkins, Baltimore, Maryland, USA, Philadelphia, Pennsylvania, USA, 423–452, 1993.
- [32] The United States Pharmacopeial Convention Uniformity of Dosage Units. Stage 6 Harmonization (905); 2011.
- [33] S. S. Spireas, Patent US6423339, 1–21, 2002.
- [34] S. M. Badr-Eldin, S. A. Elkheshen, M. M. Ghorab, *J. Drug Deliv. Sci. Technol.* **41**, 197 (2017).
- [35] N. Ahuja, O. P. Katare, B. Singh, *Eur. J. Pharm. Biopharm.* **65**, 26 (2007).
- [36] N. Chella, N. Narra, T. R. Rao, *J. Drug Deliv.* **692793**, 10 pages (2014).
- [37] M.C. Gohel, K. G. Sarvaiya, N. R. Mehta, C. D. Soni, V. U. Vyas, R. K. Dave, *Dissolution Technol.* **12**, 22 (2005).
- [38] P. Costa, *Int. J. Pharm.* **220**, 77 (2001).
- [39] V. P. Shah, Y. Tsong, P. Sathe, J. P. Liu, *Pharm. Res.* **15**, 889 (1998).
- [40] S. Spireas, S. Sadu, *Int. J. Pharm.* **166**, 177 (1998).
- [41] Y. Javadzadeh, M. R. Siahi, S. Asnaashari, A. Nokhodchi, *Acta Pharm.* **57**, 99 (2007).
- [42] H. Javaheri, P. Carter, A. A. Elkordy, *J. Pharm. Drug Dev.* **1**, 1 (2014).
- [43] N. H. Hausner, *Int. J. Powder Met.* **3**, 7 (1967).
- [44] J. N. Staniforth, M. E. Aulton, *Aulton Pharmaceutics: The design and manufacture of medicines*, Churchill Living stone Elsevier, London, 168–180, 2007.
- [45] C. Sheehan, General Chapters: <1174> Powder flow Available online: http://www.pharmacopeia.cn/v29240/usp29nf24s0_c1174.html.
- [46] V. B. Pokharkar, L. P. Mandpe, M. N. Padamwar, A. A. Ambike, K. R. Mahadik, A. Paradkar, *Powder Technol.* **167**, 20 (2006).
- [47] A. Sharma, C. P. Jain, *Res. Pharm. Sci.* **5**, 49 (2010).
- [48] R. P. Dixit, M. S. Nagarsenker, *Eur. J. Pharm. Sci.* **35**, 183 (2008).
- [49] X. Zhang, H. Xing, Y. Zhao, Z. Ma, *Pharmaceutics* **10**, 1 (2018).
- [50] L. Jagannathan, R. Meenakshi, S. Gunasekaran, S. Srinivasan, *Mol. Simul.* **36**, 283 (2010).
- [51] The United States Pharmacopeia, T.N.F. USP 28/NF 23; US Pharmacopoeial Convention Inc.: Rockville, MD, USA, 2005.
- [52] Y. Javadzadeh, L. Musaalrezaei, A. Nokhodchi, *Int. J. Pharm.* **362**, 102 (2008).
- [53] R. Dreu, S. Srčić, I. Ilić, B. Govedarica, R. Šibanc, *Int. J. Pharm.* **446**, 6 (2013).
- [54] G. Thoorens, F. Krier, B. Leclercq, B. Carlin, B. Evrard, *Int. J. Pharm.* **473**, 64 (2014).
- [55] A. A. Elkordy, X. N. Tan, E. A. Essa, *Eur. J. Pharm. Biopharm.* **83**, 203 (2013).
- [56] A. Khan, Z. Iqbal, Y. Shah, L. Ahmad, Z. Ismail, A. Ullah, *Saudi Pharm. J.* **23**, 650 (2015).
- [57] Y. Javadzadeh, M. R. Siahi-Shadbad, M. Barzegar-Jalali, A. Nokhodchi, *Farmaco* **60**, 361 (2005).
- [58] V. B. Yadav, A. V. Yadav, *J. Pharm. Sci. Res.* **1**, 44 (2009).
- [59] A. Nokhodchi, C. M. Hentzschel, C. S. Leopold, *Expert Opin. Drug Deliv.* **8**, 191 (2011).
- [60] D. S. Patel, R. M. Pipaliya, N. Surti, *Indian J. Pharm. Sci.* **77**, 290 (2015).
- [61] B. M. El-Houssieny, L. F. Wahman, N. M. S. Arafa, *Biosci. Trends* **4**, 17 (2010).
- [62] K. Adibkia, J. Shokri, M. Barzegar-Jalali, M. Solduzian, Y. Javadzadeh, *Colloids Surfaces B Biointerfaces* **113**, 10 (2014).
- [63] D. A. Diaz, S. T. Colgan, C. S. Langer, N. T. Bandi, M. D. Likar, L. Van Alstine, *AAPS J.* **18**, 15 (2016).